Hindawi
Advances in Materials Science and Engineering
Volume 2020, Article ID 9316482, 8 pages
https://doi.org/10.1155/2020/9316482

Research Article

Shear Resistance of Rock Joint under Nonuniform Normal Stress

Hang Lin,[1] **Hu Wang**,[1,2] **Yifan Chen**,[1] **Rihong Cao**,[1] **Yixian Wang**,[3] **Rui Yong**,[4] **and Shigui Du**[4]

[1]*School of Resource and Safety Engineering, Central South University, Changsha, Hunan 410083, China*
[2]*Shenzhen Municipal Design & Research Institute Co., Ltd., Shenzhen, Guangdong 518037, China*
[3]*School of Civil Engineering, Hefei University of Technology, Hefei 230009, China*
[4]*School of Civil and Environmental Engineering, Ningbo University, Ningbo, Zhejiang 315211, China*

Correspondence should be addressed to Hang Lin; linhangabc@126.com and Hu Wang; whwhclyy@163.com

Received 16 November 2019; Revised 12 February 2020; Accepted 18 February 2020; Published 23 March 2020

Academic Editor: Carlo Santulli

Many factors influence the shear resistance of rock joints. Among them, the above overburden load is the most important factor. The uneven thickness of the overburden causes the joints to be subjected to the nonuniform distribution load. While the peak shear strength shows nonlinear relationship with normal stress, linear superposition cannot be used to calculate the overall shear resistance of joint under nonuniform normal stress distribution. In this paper, the nonlinear shear strength model, JRC-JCS model, is applied to study the overall shear resistance of the joint under four nonuniform distribution patterns of normal stress. The results show that when the normal stress is distributed in a nonuniform way, the shear resistance provided by rock joint as a whole decreases with the increase of the normal stress distribution interval. Given the nonuniform distribution of normal stress along the joint, the shear resistance obtained by the Mohr-Coulomb linear model is overestimated. In order to give full play to the overall shear performance of the joint, the shear strength at different positions on the joint should be as close as possible. Then, the shear strength of joint parts can enter peak state condition simultaneously, at which time the shear strength is fully exerted.

1. Introduction

The shear behavior of rock joints is the determinate factor that controls stability of rock mass [1–6]; it has been a concern in rock mechanics and rock engineering [7–10]. Numerous joint shear strength models have been established based on experiments [11–14] and theoretical analyses [15–17]. In general, shearing along the joint surface and cutoff of asperities significantly influence shear strength. Grasselli [13], Homand et al. [16], and Zhang et al. [18] reported the relationship between shear strength and surface topography. Under shearing, stress concentration on joint surface roughness and slipping along the surface and cutoff of asperities occur simultaneously; normal stress also controls the shearing process by inhibiting the dilatation effect of the joint and affecting the contact of the rough surface; therefore, the shear strength envelope of joints represents a nonlinear characteristic [1, 19]. There are many factors influencing the shear resistance of joints in rock mass, such as thickness of overburden, joint roughness, filling condition, and occurrence of rock strata. Among them, the above overburden load is the most important factor. Due to the difference of occurrence conditions, the thickness of the joint overburden is often nonuniform, as shown in Figure 1. The uneven thickness of the overburden causes the joints to be subjected to the nonuniform distribution load, and the stress distribution of the rough body on the contact surface is affected by the uneven degree and distribution form of the overburden load [19]. To obtain the shear strength of a whole joint, shear strength should be derived at different normal stress levels. Such condition also necessitates the establishment of a nonlinear shear strength model to characterize shear behavior. A potential unstable wedge from Kangaroo Valley site in New South Wales, Australia, was recorded in a study [20, 21]; the simplified model is shown in Figure 1. Under gravity, part A features potential sliding along the joint. In the study, shear strength of joints is independent of normal stress level [21, 22], but only a portion of this

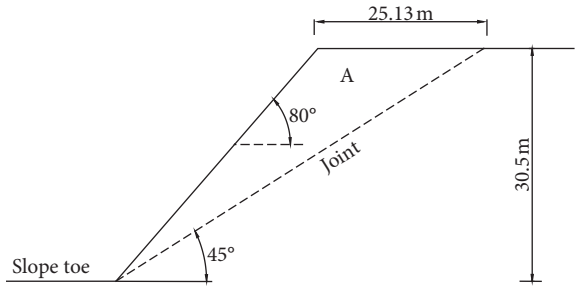

Figure 1: Simplified model of a rockslide along joint.

strength matches the characteristics of the joint surface; thus, the overall shear capacity of a joint can be obtained, and mechanical analysis can be contacted by applying the limit equilibrium method. Indraratna et al. [20] proposed a new nonlinear shear strength criterion based on JRC-JCS model, which considers the influence of normal stress level and asperity features; however, the nonuniform distribution of normal stress along the joint is not considered in its application.

Owing to the nonuniform distribution of normal stress along the joint and the nonlinear shear strength, which is closely related to joint morphology, normal stress level, and material properties [23–26], linear superposition cannot be used for shear resistance calculation of joints. The different distributions of normal stress on a joint correspond to varying degrees of shear resistance. This study investigates the shear resistance of joints based on nonlinear shear strength criterion at different nonuniform normal stress distributions. The results are compared with those of the traditional linear shear strength model, Mohr–Coulomb criterion. Progressive failure theory is then applied to determine optimal reinforcement location of joints.

2. Nonlinear Shear Behavior and Progressive Failure of Joints

The contact between the upper and lower surfaces of rock joint is closely related to normal stress and joint morphology, whereby a greater normal stress indicates a tighter contact [27–31]. Under shearing, two failure mechanisms occur through contact. In the first mechanism, the joint slips along the contact with angle α, and this mechanism is used for low normal loads (Figure 2(a)). In the second mechanism, the rough surface is plastified and breaks (Figure 2(b)), corresponding to high normal loads [1]. This mechanism subsequently forms the shear band.

According to Serrano et al. [1], in a critical slip page situation of ith contact plane, critical shear load (T_i) and critical normal load (N_i) satisfy the following relationship:

$$\frac{T_i}{N_i} = \frac{\cos\alpha_i \tan\varphi_b + \sin\alpha_i}{\cos\alpha_i - \sin\alpha_i \tan\varphi_b} = \tan\left(\varphi_b + \alpha_i\right), \quad (1)$$

where φ_b refers to basic friction angle and α_i denotes the angle between the tangential plane in ith contact and midplane of the joint.

The critical state is governed by the dip angle of the contact plane and basic friction angle. Shearing of different contact planes can occur before or during a critical state, resulting in simultaneous occurrence of shearing asperities and sliding along the contact. This phenomenon is associated with the joint material and normal stress level. Therefore, shearing of rock joint shows nonlinear characteristics. Correspondingly, progressive failure occurs with shear displacement, forming a nonlinear stress-displacement relationship (as shown in Figure 3).

Under shearing, slipping along the contact surface and cutoff of asperities occur simultaneously, and peak shear strength shows nonlinear characteristics [32]. Barton and Choubey [33] proposed an empirical law (JRC-JCS model) of friction for rock joints based on an extensive experiment on natural rock joints. In the experiment, nonlinearity is reflected by the influence of joint roughness coefficient and compressive strength on friction angle. This model is the most widely accepted in practice. From the analysis, shear strength is a nonlinear function with parameters of normal stress and joint characteristics. Although the distribution of normal stress along the joint is nonuniform in slopes or tunnels, the manner of quantifying the effect of normal stress distribution on overall shear capacity is the key for analyzing rock mass stability.

3. Shear Resistance of Joint under Nonuniform Normal Stress Distribution

3.1. Nonuniform Distribution of Normal Stress. Rock joints in slopes or tunnels considerably influence the instability of rock masses [34–37]. The destabilizing phenomenon is often sliding along the joint. Different parts of the joint correspond to different levels of normal stress, the shear strength is different, and the contribution to the overall shear resistance is also different. The existence of the joint in the slope or tunnel often makes the joint in different normal stress levels. At this state, the distribution of normal stress is nonuniform. The shear strength of the joint is a quantity related to the normal stress level and the characteristics of joint. Given the nonlinearity of shear strength, the shear capacity of joint differs at varying normal stress levels. Different joint parts correspond to different levels of normal stress and shear strength. Thus, their contributions to overall shear resistance also vary. Consequently, quantitative measurement must be performed for the normal stress distribution of the overall shear strength of joints.

3.2. Simplifying Nonuniform Normal Stress Distribution and Overall Shear Capacity. Owing to nonlinearity of shear strength and nonuniform distribution of normal stress, it is impossible to make a simple linear superposition of the overall shear strength of joint with nonuniform normal stress [19]. For linear Mohr–Coulomb criteria, linear superposition is available for shear resistance calculation and is thus independent of normal stress distribution [38–40]. Obtaining normal stress distribution on joints by analytical method presents difference. For this reason, in this study, a

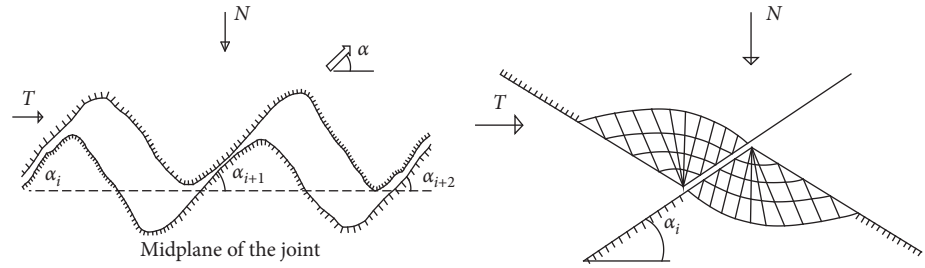

Figure 2: Two failure mechanisms of shearing along the joint (from [1]).

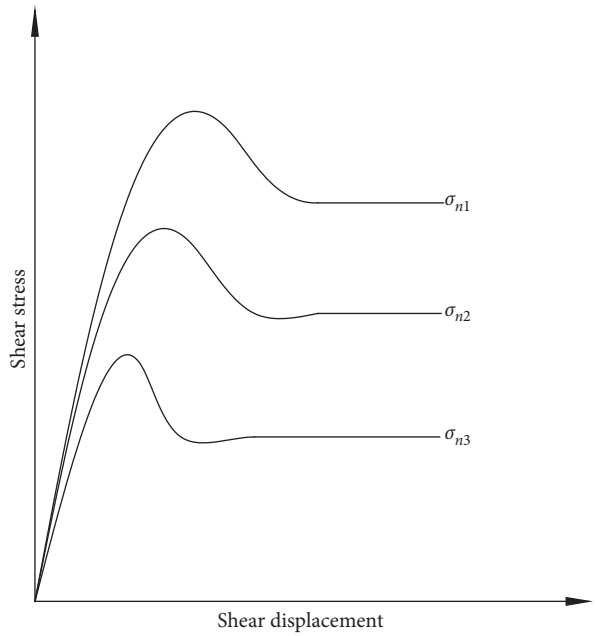

Figure 3: Progressive failure of joint under shearing ($\sigma_{n1} > \sigma_{n2} > \sigma_{n3}$).

joint submitted to four patterns of normal stress distribution, but the normal loads were the same (Figure 4). Figure 4(a) represents normal stress uniform distribution, Figure 4(b) denotes symmetric distribution, and Figures 4(c) and 4(d) are linearly increasing distributions. L and B refer to the length and width of the joint, respectively.

Let $L = 2$ m, $B = 1$ m, and $q = 1.0$ MPa; and the joint properties are the same with joint J-II by Hu et al. [41]; that is, JCS is 27.5 MPa, JRC is 16.5, and residual friction angle is 35°. Cohesion and friction measure 0.82 MPa and 41.51°, respectively, as described by the Mohr–Coulomb criteria. Therefore, peak shear strength of the joint can be determined by JRC-JCS model and Mohr–Coulomb criteria, respectively, as follows:

$$\tau = \sigma_n \tan\left[35 + 16.5 \log\left(\frac{27.5}{\sigma_n}\right)\right],$$
$$\tau = 0.82 + 0.885\sigma_n, \tag{2}$$

where τ represents peak shear strength (MPa); σ_n denotes normal stress (MPa).

Under shearing, the joint is at the ultimate state. The overall shear resistance (unit: MN) of the joint can be obtained by the JRC-JCS model and Mohr–Coulomb criteria, respectively, as follows:

$$F = \int_L \sigma_n \tan\left[35 + 16.5 \log\left(\frac{27.5}{\sigma_n}\right)\right] \mathrm{d}L, \tag{3}$$

$$F = \int_L \sigma_n (0.82 + 0.885\sigma_n) \mathrm{d}L, \tag{4}$$

where L denotes the length of joint.

In Figure 4(a), $\sigma_n = q = 1$ MPa, and the shear resistance of the joint from JRC-JCS model is as follows:

$$F = \int_L \tan\left[35 + 16.5 \log\left(\frac{27.5}{1}\right)\right] \mathrm{d}L = 3.2958. \tag{5}$$

In Figure 4(b), the distribution of normal stressσ_n, can be obtained with the following expression:

$$\sigma_n = \begin{cases} -x + 1.5q, & 0 \le x \le \dfrac{L}{2}, \\ x + 1.5q, & -\dfrac{L}{2} \le x < 0. \end{cases} \tag{6}$$

Substituting (6) into (3), the shear resistance is computed as follows:

$$F = \int_0^{L/2} (-x + 1.5q) \tan\left[35 + 16.5 \log\left(\frac{27.5}{-x + 1.5q}\right)\right] \mathrm{d}L + \int_{-L/2}^{0} (x + 1.5q) \tan\left[35 + 16.5 \log\left(\frac{27.5}{x + 1.5q}\right)\right] \mathrm{d}L = 3.2722. \tag{7}$$

In Figure 4(c), the normal stress distribution can be obtained with the following expression:

$$\sigma_n = -\frac{1}{2}x + 1.5q, \quad 0 \le x < L. \tag{8}$$

Substituting (8) into (3), we obtain the shear resistance as follows:

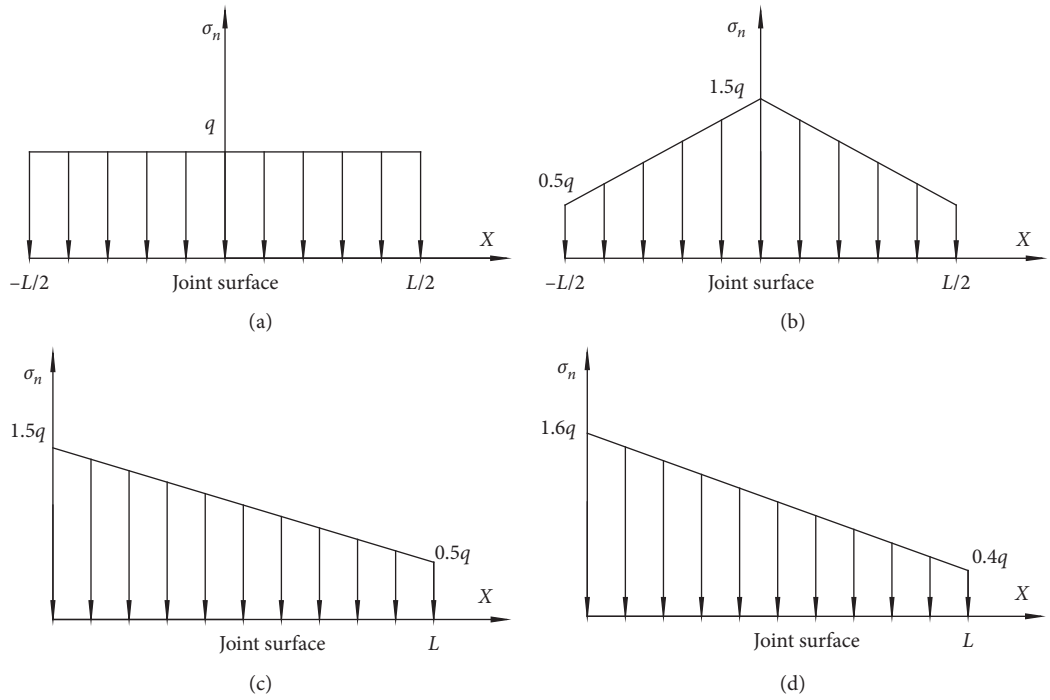

Figure 4: Distribution patterns of normal stress along the joint surface (where $q = 1.0$ Mpa). (a) Uniform distribution. (b) Symmetric distribution. (c) Linear distribution. (d) Linear distribution.

$$F = \int_0^L \left(-\frac{1}{2}x + 1.5q\right)\tan\left[35 + 16.5\log\left(\frac{27.5}{-1/2x + 1.5q}\right)\right]\mathrm{d}L = 3.2722. \tag{9}$$

In Figure 4(d), the normal stress distribution can be obtained with the following expression:

$$\sigma_n = -0.6x + 1.6q, \quad 0 \le x \le L. \tag{10}$$

Substituting (10) into (3), the shear resistance is calculated as follows:

$$F = \int_0^L (-0.6x + 1.6q)\tan\left[35 + 16.5\log\left(\frac{27.5}{-0.6x + 1.6q}\right)\right]\mathrm{d}L = 3.2612. \tag{11}$$

The Mohr–Coulomb model is a linear model, and shear resistance can be obtained by linear superposition of shear strength [42, 43]. Hence, shear resistance is determined by normal load and not based on the distribution of normal stress. Under the same normal load, the results of the JRC-JCS model show that shear resistance provided by the whole structure decreases with increasing normal stress interval, shown in Table 1. If the results of the first distribution (uniform distribution) are taken as the standard, the results of the other three distributions are 0.72%, 0.72%, and 1.1% less than those of the first distribution, respectively. The shear resistance of a joint was determined by the length of joint, shear strength (linearity and nonlinearity), and normal stress. However, the larger the normal stress and the length, the larger the difference. Owing to the nonuniform distribution of normal stress in practice, the shear resistance obtained by the Mohr–Coulomb linear model is overestimated. Considering the nonlinear shear behavior of rock joint, adopting the nonlinear shear strength model is necessary, and it is essential to specify the normal stress distribution on joint surface. At different normal stress levels, the shear strength of joint is different. When the normal stress is distributed in a nonuniform way, the shear resistance provided by rock joint as a whole decreases with the increase of the normal stress distribution interval. In addition, when the level of normal stress is very low, the JRC-JCS model presents an uncomputable situation, where $\tan[\phi_r + \mathrm{JRClog}(\mathrm{JCS}/\sigma_n)]$ is an oscillatory function.

4. Optimization of Reinforcement Position

The deterioration of shear resistance in rock joints often leads to engineering failure, such as slope sliding, which endangers the safety of engineering. Therefore, it is very important to reinforce the rock joint [44, 45]. Under shearing, progressive failure occurs in rock joints. With shear displacement, shear strength first increases to peak strength and then approaches residual strength [46–48]. However, normal stress on the joint shows no uniform distribution. On the basis of nonlinear shear strength, at different positions, stress can occur before or during peak intensity (critical state) and possibly at the residual strength stage. Asadollahi and Tonon [7] showed that the increase in normal stress on joint increases displacement of the joint reaching the peak shear strength, as shown in Figure 3.

Table 1: Comparison of overall shear resistance of a joint with different normal stress distribution patterns.

Normal stress distribution	Overall shear resistance (unit: MN)			
	Uniform distribution (a)	Symmetric distribution (b)	Linearly increasing distribution (c)	Linearly increasing distribution (d)
M-C	3.41	3.41	3.41	3.41
JRC-JCS model	3.2958	3.2722	3.2722	3.2612

Table 2: Shear strength at different normal stress levels.

Normal stress (MPa)	Shear strength (MPa)	
	M-C	JRC-JCS
1.6	2.24	2.32
1.5	2.15	2.21
1.0	1.71	1.65
0.5	1.26	1.01
0.4	1.17	0.87

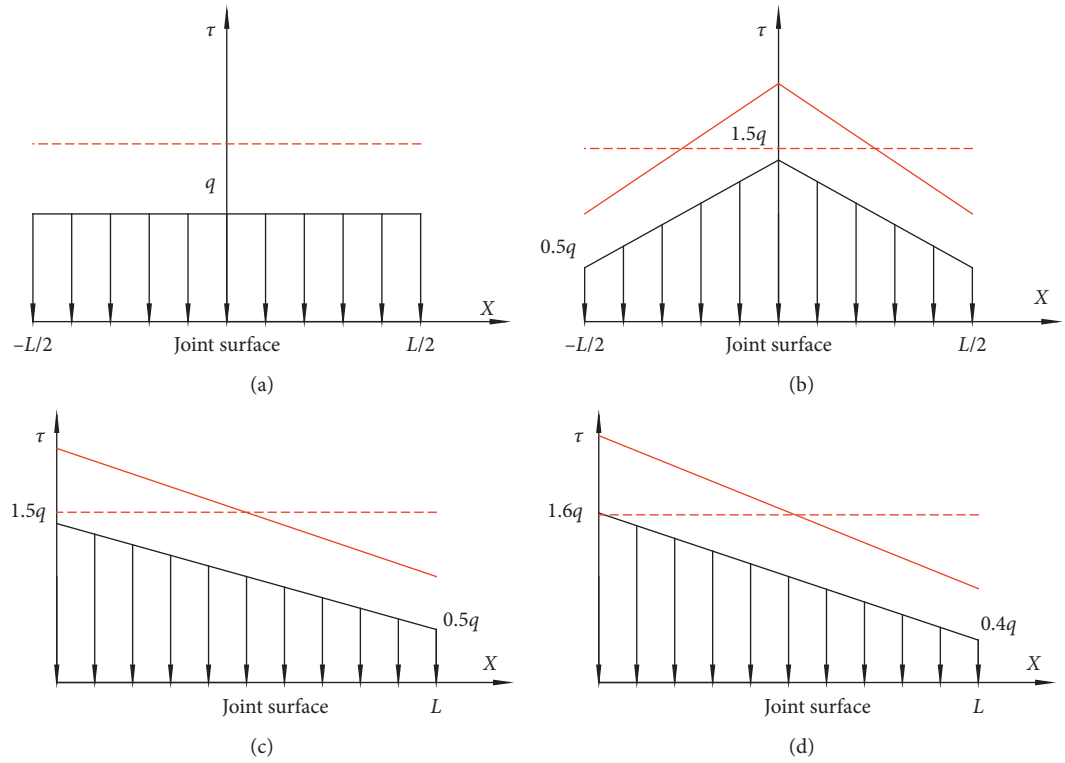

Figure 5: Peak shear strength and the average shear strength of the joint in JRC-JCS model (peak shear strength: the solid red line; average shear strength: the dashed red line). (a) Uniform distribution. (b) Symmetric distribution. (c) Linear distribution. (d) Linear distribution.

Slope stability analysis methods, such as the common limit equilibrium and strength reduction, are based on limit state under the assumption that sliding zoom is at critical state [49–52]. In practice, the state may be observed before or after the peak state, resulting in failure to satisfy this assumption. As summed up by Huang [53], the typical geomechanical models of landslides in rocks, including the "three sections" (i.e., sliding-tension cracking-shearing), "retaining wall collapse," and creep-bending-shearing model, indicate that different parts of rock develop in varied shear states during landslide inoculation. In the slope treatment of potential instability along the joint, the joint should avoid partial transition into progressive failure, which requires control of the entire progressive failure process. The normal stress of the joint or potential slip zone of the slope is nonuniform and the shear strength provided by different positions is not the same. The potential sliding trend is generated under the action of gravity, and the shear resistance provided by the joint as a whole is used to overcome the sliding force.

Assuming that reinforcement is used to improve normal stress on the joint surface in Figure 4, the same increment of

normal stress will result in different increments of shear strength considering the nonlinearity of shear strength. When normal stress is smaller, the increase of shear strength is higher for the same increment of normal stress (as listed in Table 2), which is more conducive to the improvement of overall shear resistance. Considering the nonlinear shear strength behavior of joint independently and when the reinforcement method is used to improve the normal stress level of the structural surface, then reinforcement is loaded at location with a lower original normal stress level and better results are obtained. However, from the theory of progressive failure, under shear load with certain shear displacement, the front edge of the structure has reached the peak state, whereas the back edge has shown otherwise. At this point, the joint can remain stable. When shear load is sufficiently large, the front edge of the structure reaches the residual strength stage after adequate shear displacement, and the back edge reaches the peak stage slowly. In this case, the shear resistance of the structural surface has not fully developed as it is not entirely at the peak shear state. To maximize the shear capability of the joint, the shear stress shear displacement curves should be closely located (Figure 3) for the different parts of the joint to avoid progressive failure.

Based on the JRC-JCS model, the distribution of shear strength on the joint surface under nonuniform stress distribution is obtained, as shown in Figure 5 and Table 2, in which peak shear strength and average shear strength are presented in solid red and dashed red lines, respectively. According to the above analysis, reinforcement should be located in the area where peak shear strength approaches average shear strength; that is, the vicinity of the solid red line intersects the dashed red line (as shown in Figure 5). Under the action of shear force, part of the joint produces a certain shear displacement, and different positions of the joint are close to each other on the shear stress shear displacement curve. Then, the shear strength of joint parts can effectively avoid entering the residual state, at which time the shear strength is fully exerted.

Joint reinforcement should be considered from two aspects: nonlinear shear strength and progressive failure along the joint. In nonlinear shear criterion, a lower original normal stress level causes more significant marginal effect of shear resistance for the same increment of normal stress. In addition, progressive failure along the joint should also be avoided. Reinforcement should cause the shear capacity of joint to lie close to the region where peak shear strength is near the average value. Consequently, the shear curves at different positions of the joint are closely located, and then joint parts enter peak state condition simultaneously under shearing, to achieve full shear capacity.

5. Conclusions

(1) Due to the difference of occurrence conditions, the thickness of the joint overburden is often nonuniform. Different parts of the joint correspond to different levels of normal stress, the shear strength is different, and the contribution to the overall shear resistance is also different.

(2) When the normal stress is distributed in a nonuniform way, the shear resistance provided by rock joint as a whole decreases with the increase of the normal stress distribution interval. Given the nonuniform distribution of normal stress along the joint in practice, the shear resistance obtained by the Mohr–Coulomb linear model is overestimated.

(3) In order to give full play to the overall shear performance of the joint, the shear strength at different positions on the joint should be as close as possible. Then, the shear strength of joint parts can enter peak state condition simultaneously, at which time the shear strength is fully exerted.

Data Availability

The data used to support the findings of this study are available from the corresponding author upon request.

Conflicts of Interest

The authors declare no conflicts of interest.

Acknowledgments

This paper gets its funding from projects (51774107, 51774322, and 51774131) supported by the National Natural Science Foundation of China and project (2018JJ2500) supported by Hunan Provincial Natural Science Foundation of China. The authors wish to acknowledge these supports.

References

[1] A. Serrano, C. Olalla, and R. A. Galindo, "Micromechanical basis for shear strength of rock discontinuities," *International Journal of Rock Mechanics and Mining Sciences*, vol. 70, pp. 33–46, 2014.

[2] C. O. Aksoy, O. Kantarci, and V. Ozacar, "An example of estimating rock mass deformation around an underground opening using numerical modeling," *International Journal of Rock Mechanics and Mining Sciences*, vol. 47, no. 2, pp. 272–278, 2010.

[3] W. Wan, J. Liu, and J. Liu, "Effects of asperity angle and infill thickness on shear characteristics under constant normal load conditions," *Geotechnical and Geological Engineering*, vol. 36, no. 4, pp. 2761–2767, 2018.

[4] J. Shen, M. Karakus, and C. Xu, "Direct expressions for linearization of shear strength envelopes given by the Generalized Hoek-Brown criterion using genetic programming," *Computers and Geotechnics*, vol. 44, pp. 139–146, 2012.

[5] Y. Zhao, J. Tang, Y. Chen et al., "Hydromechanical coupling tests for mechanical and permeability characteristics of fractured limestone in complete stress-strain process," *Environmental Earth Sciences*, vol. 76, no. 1, p. 24, 2017.

[6] H. Lin, P. Sun, Y. Chen, Y. Zhu, X. Fan, and Y. Zhao, "Analytical and experimental analysis of the shear strength of bolted saw-tooth joints," *European Journal of Environmental and Civil Engineering*, vol. 24, pp. 1–15, 2020.

[7] P. Asadollahi and F. Tonon, "Constitutive model for rock fractures: revisiting Barton's empirical model," *Engineering Geology*, vol. 113, no. 1–4, pp. 11–32, 2010.

[8] M. Bahaaddini, G. Sharrock, and B. K. Hebblewhite, "Numerical investigation of the effect of joint geometrical parameters on the mechanical properties of a non-persistent jointed rock mass under uniaxial compression," *Computers and Geotechnics*, vol. 49, pp. 206–225, 2013.

[9] R. Yong, J.-B. Qin, M. Huang, S.-G. Du, J. Liu, and G.-J. Hu, "An innovative sampling method for determining the scale effect of rock joints," *Rock Mechanics and Rock Engineering*, vol. 52, no. 3, pp. 935–946, 2018.

[10] H. Lin, S. Xie, R. Yong, Y. Chen, and S. Du, "An empirical statistical constitutive relationship for rock joint shearing considering scale effect," *Comptes Rendus Mécanique*, vol. 347, no. 8, pp. 561–575, 2019.

[11] J. Yang, G. Rong, D. Hou, J. Peng, and C. Zhou, "Experimental study on peak shear strength criterion for rock joints," *Rock Mechanics and Rock Engineering*, vol. 49, no. 3, pp. 821–835, 2016.

[12] C.-C. Xia, Z.-C. Tang, W.-M. Xiao, and Y.-L. Song, "New peak shear strength criterion of rock joints based on quantified surface description," *Rock Mechanics and Rock Engineering*, vol. 47, no. 2, pp. 387–400, 2014.

[13] G. Grasselli, "Manuel rocha medal recipient shear strength of rock joints based on quantified surface description," *Rock Mechanics and Rock Engineering*, vol. 39, no. 4, pp. 295–314, 2006.

[14] S. Xie, H. Lin, Y. Wang et al., "A statistical damage constitutive model considering whole joint shear deformation," *International Journal of Damage Mechanics*, vol. 29, 2020.

[15] S. Xie, H. Lin, Y. Chen, R. Yong, W. Xiong, and S. Du, "A damage constitutive model for shear behavior of joints based on determination of the yield point," *International Journal of Rock Mechanics and Mining Sciences*, vol. 128, Article ID 104269, 2020.

[16] F. Homand, T. Belem, and M. Souley, "Friction and degradation of rock joint surfaces under shear loads," *International Journal for Numerical and Analytical Methods in Geomechanics*, vol. 25, no. 10, pp. 973–999, 2001.

[17] W. Yang, G. Li, P. Ranjith, and L. Fang, "An experimental study of mechanical behavior of brittle rock-like specimens with multi-non-persistent joints under uniaxial compression and damage analysis," *International Journal of Damage Mechanics*, vol. 28, no. 10, pp. 1490–1522, 2019.

[18] X. Zhang, Q. Jiang, N. Chen, W. Wei, and X. Feng, "Laboratory investigation on shear behavior of rock joints and a new peak shear strength criterion," *Rock Mechanics & Rock Engineering*, vol. 49, no. 9, pp. 3495–3512, 2016.

[19] H. Wang and H. Lin, "Non-linear shear strength criterion for a rock joint with consideration of friction variation," *Geotechnical and Geological Engineering*, vol. 36, no. 6, pp. 3731–3741, 2018.

[20] B. Indraratna, W. Premadasa, E. T. Brown, A. Gens, and A. Heitor, "Shear strength of rock joints influenced by compacted infill," *International Journal of Rock Mechanics and Mining Sciences*, vol. 70, pp. 296–307, 2014.

[21] D. A. F. Oliveira, B. Indraratna, and J. Nemcik, "Critical review on shear strength models for soil-infilled joints," *Geomechanics and Geoengineering*, vol. 4, no. 3, pp. 237–244, 2009.

[22] H. Lin, X. Ding, R. Yong, W. Xu, and S. Du, "Effect of non-persistent joints distribution on shear behavior," *Comptes Rendus Mécanique*, vol. 347, no. 6, pp. 477–489, 2019.

[23] M. Naderloo, M. Moosavi, and M. Ahmadi, "Using acoustic emission technique to monitor damage progress around joints in brittle materials," *Theoretical and Applied Fracture Mechanics*, vol. 104, Article ID 102368, 2019.

[24] J. Liu, Y. Chen, W. Wan, J. Wang, and X. Fan, "The influence of bedding plane orientation on rock breakages in biaxial states," *Theoretical and Applied Fracture Mechanics*, vol. 95, pp. 186–193, 2018.

[25] Y. H. Huang, S. Q. Yang, and W. L. Tian, "Cracking process of a granite specimen that contains multiple pre-existing holes under uniaxial compression," *Fatigue & Fracture of Engineering Materials & Structures*, vol. 42, no. 6, pp. 1341–1356, 2019.

[26] S.-Q. Yang, P.-F. Yin, Y.-C. Zhang et al., "Failure behavior and crack evolution mechanism of a non-persistent jointed rock mass containing a circular hole," *International Journal of Rock Mechanics and Mining Sciences*, vol. 114, pp. 101–121, 2019.

[27] M. Wang, P. Cao, and Y. Chen, "Anisotropy of rock profile JRC values and its empirical formula: a case study on yellow rust granite," *Geotechnical and Geological Engineering*, vol. 35, no. 4, pp. 1645–1655, 2017.

[28] C. Zhang, H. Lin, C. Qiu, T. Jiang, and J. Zhang, "The effect of cross-section shape on deformation, damage and failure of rock-like materials under uniaxial compression from both a macro and micro viewpoint," *International Journal of Damage Mechanics*, vol. 20, 2020.

[29] Y. Wang, H. Zhang, H. Lin, Y. Zhao, and Y. Liu, "Fracture behaviour of central-flawed rock plate under uniaxial compression," *Theoretical and Applied Fracture Mechanics*, vol. 106, Article ID 102503, 2020.

[30] H. Chen, X. Fan, H. Lai, Y. Xie, and Z. He, "Experimental and numerical study of granite blocks containing two side flaws and a tunnel-shaped opening," *Theoretical and Applied Fracture Mechanics*, vol. 104, Article ID 102394, 2019.

[31] Y. Zhao, Y. Wang, W. Wang, L. Tang, Q. Liu, and G. Cheng, "Modeling of rheological fracture behavior of rock cracks subjected to hydraulic pressure and far field stresses," *Theoretical and Applied Fracture Mechanics*, vol. 101, pp. 59–66, 2019.

[32] N. Barton, "Shear strength criteria for rock, rock joints, rockfill and rock masses: problems and some solutions," *Journal of Rock Mechanics and Geotechnical Engineering*, vol. 5, no. 4, pp. 249–261, 2013.

[33] N. Barton and V. Choubey, "The shear strength of rock joints in theory and practice," *Rock Mechanics Felsmechanik Mecanique des Roches*, vol. 10, no. 1-2, pp. 1–54, 1977.

[34] Y. Wang, H. Lin, Y. Zhao, X. Li, P. Guo, and Y. Liu, "Analysis of fracturing characteristics of unconfined rock plate under edge-on impact loading," *European Journal of Environmental and Civil Engineering*, vol. 23, pp. 1–16, 2019.

[35] F. Dai, Y. Xu, T. Zhao, N.-W. Xu, and Y. Liu, "Loading-rate-dependent progressive fracturing of cracked chevron-notched Brazilian disc specimens in split Hopkinson pressure bar tests," *International Journal of Rock Mechanics and Mining Sciences*, vol. 88, pp. 49–60, 2016.

[36] C. Zhang, C. Pu, R. Cao, T. Jiang, and G. Huang, "The stability and roof-support optimization of roadways passing through unfavorable geological bodies using advanced detection and monitoring methods, among others, in the Sanmenxia Bauxite Mine in China's Henan Province," *Bulletin of Engineering Geology and the Environment*, vol. 78, no. 7, pp. 5087–5099, 2019.

[37] H. Lin, H. Yang, Y. Wang, Y. Zhao, and R. Cao, "Determination of the stress field and crack initiation angle of an open flaw tip under uniaxial compression," *Theoretical and Applied Fracture Mechanics*, vol. 104, Article ID 102358, 2019.

[38] Q. Zhang, B. S. Jiang, X. S. Wu, H. Q. Zhang, and L. J. Han, "Elasto-plastic coupling analysis of circular openings in elasto-brittle-plastic rock mass," *Theoretical and Applied Fracture Mechanics*, vol. 60, no. 1, pp. 60–67, 2012.

[39] Y.-H. Huang and S.-Q. Yang, "Mechanical and cracking behavior of granite containing two coplanar flaws under conventional triaxial compression," *International Journal of Damage Mechanics*, vol. 28, no. 4, pp. 590–610, 2018.

[40] D. Lei, H. Lin, Y. Chen, R. Cao, and Z. Wen, "Effect of cyclic freezing-thawing on the shear mechanical characteristics of nonpersistent joints," *Advances in Materials Science and Engineering*, vol. 2019, Article ID 9867681, 14 pages, 2019.

[41] L. M. Hu, M. A. Jie, and B. Y. Zhang, "Numerical simulation of interface failure during direct shear tests," *Journal of Tsinghua University*, vol. 48, pp. 943–946, 2008.

[42] S. Nesrine, J. Mouad, M. Etienne et al., "Identification of a cohesive zone model for cement paste-aggregate interface in a shear test," *European Journal of Environmental and Civil Engineering*, vol. 23, pp. 1–15, 2019.

[43] F. Prunier and D. Branque, "Definition of a safety factor using the finite element method in geomechanics, from a static to dynamic regime," *European Journal of Environmental and Civil Engineering*, vol. 23, pp. 1–22, 2019.

[44] H. Lin, Y. Zhu, J. Yang, and Z. Wen, "Anchor stress and deformation of the bolted joint under shearing," *Advances in Civil Engineering*, vol. 2020, Article ID 3696489, 10 pages, 2020.

[45] G. Tiwari and G. M. Latha, "Stability analysis and design of stabilization measures for chenab railway bridge rock slopes," *Bulletin of Engineering Geology and the Environment*, vol. 79, no. 2, pp. 603–627, 2019.

[46] K. Zhang, P. Tan, G. Ma, and P. Cao, "Modeling of the progressive failure of an overhang slope subject to differential weathering in three gorges reservoir, China," *Landslides*, vol. 13, no. 5, pp. 1–11, 2015.

[47] M. Bahaaddini, A. M. Sheikhpourkhani, and H. Mansouri, "Flat-joint model to reproduce the mechanical behaviour of intact rocks," *European Journal of Environmental and Civil Engineering*, vol. 23, pp. 1–22, 2019.

[48] R. Yong, J. Ye, S.-G. Du, H. Zhang, L. Gu, and H. Lin, "A dice similarity measure for TBM penetrability classification in hard rock condition with the intuitionistic fuzzy information of rock mass properties," *European Journal of Environmental and Civil Engineering*, vol. 23, pp. 1–16, 2019.

[49] Y. Chen and H. Lin, "Consistency analysis of Hoek-Brown and equivalent Mohr-coulomb parameters in calculating slope safety factor," *Bulletin of Engineering Geology and the Environment*, vol. 78, no. 6, pp. 4349–4361, 2019.

[50] M. R. Arvin, A. Zakeri, and M. Bahmani Shoorijeh, "Using finite element strength reduction method for stability analysis of geocell-reinforced slopes," *Geotechnical and Geological Engineering*, vol. 37, no. 3, pp. 1453–1467, 2019.

[51] J. Zhang and J. Li, "A comparative study between infinite slope model and Bishop's method for the shallow slope stability evaluation," *European Journal of Environmental and Civil Engineering*, vol. 37, pp. 1–18, 2019.

[52] W. Yuan, J. Li, Z. Li, W. Wang, and X. Sun, "A strength reduction method based on the Generalized Hoek-Brown (GHB) criterion for rock slope stability analysis," *Computers and Geotechnics*, vol. 117, Article ID 103240, 2020.

[53] R. Huang, "Large-scale landslides and their sliding mechanisms in China since the 20th century," *Chinese Journal of Rock Mechanics & Engineering*, vol. 26, pp. 433–454, 2007.